Rev. Roum. Sci. Techn.– Électrotechn. et Énerg.
Vol. **62**, *4*, pp. 399–404, Bucarest, 2017

MICROWAVE BANDPASS FILTERS WITH OPEN-LOOP TRIANGULAR MICROSTRIP RESONATORS

NICOLAE MILITARU, DIANA BUCUR

Key words: Resonator, Microstrip technology, Bandpass filters, Couplings, Microwaves.

This paper presents the design of novel microwave bandpass filters, composed of coupled single-mode triangular resonators, in microstrip technology. Based on the study through electromagnetic-field simulation on the couplings between pairs of such open-loop triangular resonators and between a single resonator and its 50 Ω feeding line, microwave bandpass filters with various specifications can be developed, for telecommunications and radar applications. Here, two bandpass filters with different types of couplings between resonators are designed, fabricated and tested. The electrical performances of the experimental models meet the specification, which validates and proves the flexibility of the design of bandpass filters composed of coupled triangular microstrip resonators.

1. INTRODUCTION

Planar bandpass filters represent important elements of many telecommunication systems (including, here, mobile communications, specific equipment, and radar systems), operating in the RF/microwave spectrum [1]. The requirements of such filters depend on the application in question and they can refer to some electrical performance of these filtering structures, such as insertion loss, selectivity, bandwidth, group-delay response in the passband, and, also, to some other aspects like size and cost.

In order to obtain different filtering characteristics and small dimensions, the current published contributions in the field demonstrate different microstrip geometries for the bandpass filters' resonators [2–6] and various coupling scheme in planar technology (microstrip, multilayer) between these resonators [7–14]. The design – in almost all its stages – of such planar filters involves the use of electromagnetic-field simulation and optimization, which is a difficult task.

In this context, the paper proposes a new type of open-loop microstrip resonator, with a triangular shape, in the design of microwave bandpass filters. The use of such resonator leads to the possibility of obtaining bandpass filters with different coupling topologies – and hence, different electrical characteristics – either in microstrip or in multilayer technologies.

Based on this type of resonator, several configurations of microstrip bandpass filters are designed, analyzed, fabricated and tested.

The electrical performance of the proposed filters are compared to the measured characteristics of the corresponding experimental models. It is noticed a good agreement, which validates the design and demonstrates its flexibility.

2. TRIANGULAR MICROSTRIP RESONATOR AND COUPLING TOPOLOGIES

The proposed triangular microstrip resonator was designed for applications in the 3.5 GHz frequency band, using a Rogers RO3003™ substrate with a dielectric constant ε_r of 3, substrate height h of 0.508 mm, dielectric loss tangent tanδ of 0.001, and two electrodeposited copper foils with a thickness t of 0.017 mm.

Figure 1 provides the dimensions of the resonator, obtained through electromagnetic-field simulation [15], so that its first resonance be at 3.5 GHz, and the frequency response of the resonator, at resonance.

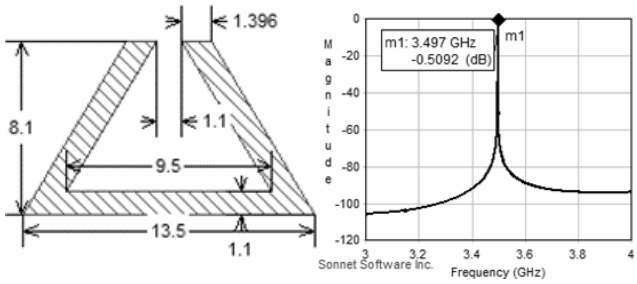

a) b)

Fig. 1 – The proposed triangular microstrip resonator: a) layout (unit: mm); b) $|S_{21}|$ [dB] frequency response at 3.5 GHz.

The small difference between 3.5 GHz and the actual resonant frequency, 3.497 GHz, (as depicted in Fig. 1b) is a result of the resolution (0.1 mm) used in the layout editor [15].

Based on the current density distribution inside the resonator, different types of couplings between a resonator and its 50 Ω feeding line (I/O coupling) and between a pair of triangular resonators were investigated through electro-magnetic-field simulation.

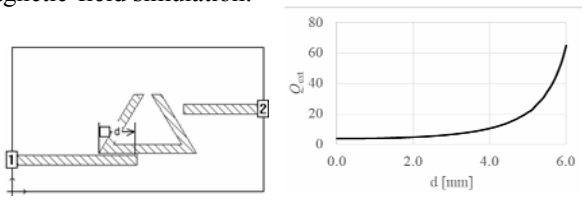

a) b)

Fig. 2 – Coupling resonator – feeding line: a) configuration; b) the external quality factor, Q_{ext}, *vs*. feeding line.

Different values of the external quality factor Q_{ext} – which characterizes this type of coupling – can be obtained by changing the coupling position (parameter d in Fig. 1a) of the 50 Ω feeding line in relation to the resonator.

Considering the proposed configuration in Fig. 1a – which correspond to a doubly loaded resonator – the external quality factor Q_{ext} of the lossless resonator can be derived from its frequency response $|S_{21}|$ [dB], with [1]:

"Politehnica" University of Bucharest, 313 Splaiul Independentei, Bucharest, Romania, E-mail: nicolae.militaru@upb.ro

$$Q_{\text{ext}} = \frac{f_0}{B_{3\text{dB}}}, \tag{1}$$

where f_0 is the resonant frequency and $B_{3\text{dB}}$ represents the bandwidth for which the resonant amplitude response $|S_{21}|$ [dB] is up 3 dB from that at resonance.

From Fig. 2b it can be noticed the dependence of Q_{ext} with the parameter *d*.

Using the proposed microstrip resonator, different couplings between a pair of such resonators can be obtained. These couplings are presented in the Figs. 3–5.

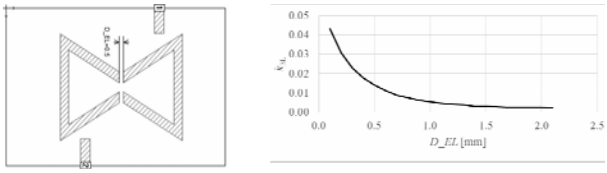

a) b)

Fig. 3 – Electric coupling structure: a) microstrip configuration; b) coupling coefficient k_{EL} *vs.* distance *D_EL* between resonators.

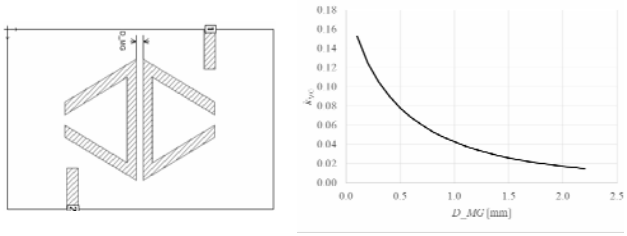

a) b)

Fig. 4 – Magnetic coupling structure; a) microstrip configuration; b) coupling coefficient k_{MG} *vs.* distance *D_MG* between resonators.

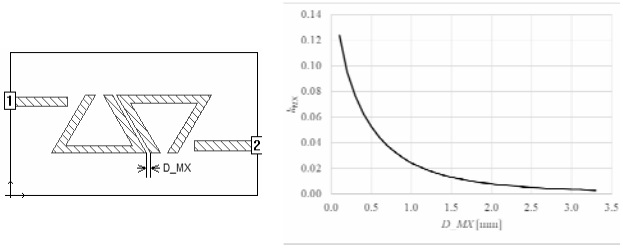

a) b)

Fig. 5 – Type-I mixed coupling structure: a) microstrip configuration; b) coupling coefficient k_{MX} *vs.* distance *D_MX* between resonators.

For each particular distance between resonators, the coupling coefficient *k* was computed based on the response of the coupled resonators, using [1]:

$$k = \frac{f_{p2}^2 - f_{p1}^2}{f_{p2}^2 + f_{p1}^2}, \tag{2}$$

where f_{p1} and f_{p2} are the two resonant peaks that correspond to the characteristic frequencies extracted from the resonant response $|S_{21}|$ [dB] of coupled resonator structure [1].

The responses from Figs. 3b–5b show that coupling coefficient *k* decreases with the distance between resonators.

The above results, obtained through electromagnetic-field simulation, are used in the stage of the design where the microstrip layout of the bandpass filters are generated, as detailed hereafter.

3. DESIGN OF FILTERS

The results from previous section allow designing of various microstrip bandpass filters with coupled triangular resonators.

Two novel microstrip bandpass filters are proposed in this paper. Both filtering structures have the same topology, shown in Fig. 6, but different coupling configurations between two consecutive resonators.

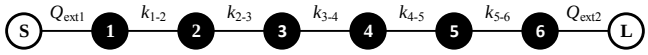

Fig. 6 – Topology of six-coupled resonators, corresponding to a sixth-order bandpass filter.

Both bandpass filters are design to meet the same specification:

- Filter's order: $n = 6$.
- Center frequency: $f_0 = 3.5$ GHz.
- Passband bandwidth: $B = 200$ MHz (fractional bandwidth FBW = 0.057).
- Chebyshev characteristic, with a passband ripple.
- Source and load reference impedance: $Z_0 = 50\ \Omega$;

The filters are designed using the dielectric substrate and metallization detailed in Section 2.

Based on the specification, the normalized values for Chebyshev lowpass prototype filters having $g_0 = 1$ and responses with 0.5 dB ripple are [1]:

Table 1

Normalized values for Chebyshev lowpass prototype filters, $R = 0.5$ dB

g_0	g_1	g_2	g_3	g_4	g_5	g_6	g_7
1	1.7254	1.2479	2.6064	1.3137	2.4758	0.8696	1.9841

Using the values in Table 1 one gets [1] the necessary external quality factors

$$Q_{\text{ext1}} = \frac{g_0 g_1}{\text{FBW}} = 30.195, \tag{3}$$

$$Q_{\text{ext2}} = \frac{g_6 g_7}{\text{FBW}} = 30.194 \cong Q_{\text{ext1}} \overset{\text{not}}{=} Q_{\text{ext}}, \tag{4}$$

and the necessary coupling coefficients:

$$k_{1-2} = \frac{\text{FBW}}{\sqrt{g_1 g_2}} = 0.038943, \tag{5}$$

$$k_{2-3} = \frac{\text{FBW}}{\sqrt{g_2 g_3}} = 0.031685, \tag{6}$$

$$k_{3-4} = \frac{\text{FBW}}{\sqrt{g_3 g_4}} = 0.030881, \tag{7}$$

$$k_{4-5} = \frac{\text{FBW}}{\sqrt{g_4 g_5}} = 0.031685 = k_{2-3}, \tag{8}$$

$$k_{5-6} = \frac{\text{FBW}}{\sqrt{g_5 g_6}} = 0.038944 \cong k_{1-2}. \tag{9}$$

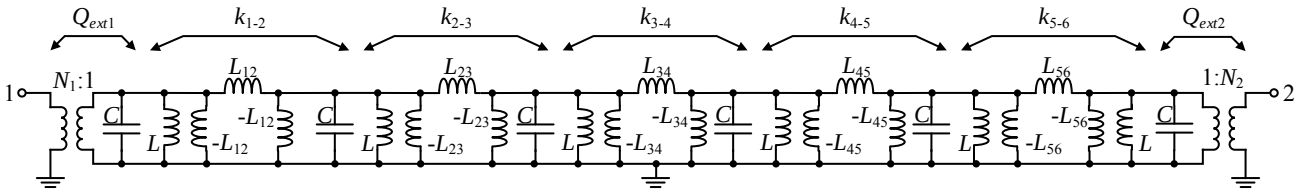

Fig. 7 – Lossless lumped-elements circuit model
for the proposed sixth-order bandpass filters.

Table 2

Values of the reactive components from Fig. 7

C	$L=\frac{1}{4\pi^2 f_0^2 C}$	$N=\sqrt{\frac{2\pi f_0 Z_0 C}{Q_{ext}}}$	$L_{12}=\frac{L}{k_{1-2}}$	$L_{23}=\frac{L}{k_{2-3}}$	$L_{34}=\frac{L}{k_{3-4}}$	$L_{45}=\frac{L}{k_{4-5}}$	$L_{56}=\frac{L}{k_{5-6}}$
1 pF	2.067 nH	0.1908	53.0978 nH	65.2608 nH	66.9592 nH	65.2601 nH	53.0957 nH

The values of the reactive elements from Fig. 7 are shown in Table 2. Two ideal transformers with practically identical turns ratios $N_1 = N_2 = N$ provides source – first resonant circuit and last resonant circuit – load couplings.

There are six lossless 3.5 GHz synchronously-tuned parallel LC resonant circuits, corresponding to the filters' order. The L_{ij} lossless inductors provide the necessary coupling between two consecutive lossless LC resonant circuits.

The frequency response of the circuit model from Fig. 7, obtained with the aid of a linear circuit simulator [16], is shown in Fig. 8.

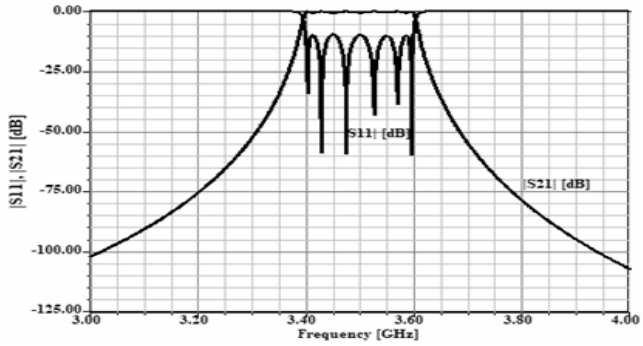

Fig. 8 – Frequency response of the bandpass filter from Fig. 7.

It is noticed that reflection and transmission characteristics of the circuit model from Fig. 7 meet the specification, which validates the circuit model design.

Based on the coupling topology from Fig. 6, two different types of microstrip bandpass filters with coupled triangular resonators are proposed.

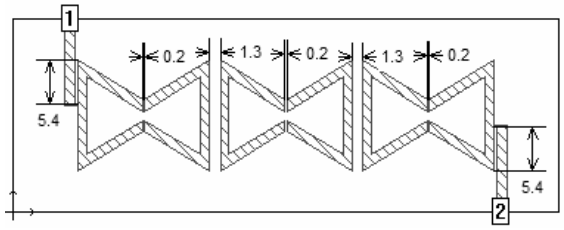

Fig. 9 – Type 1 microwave sixth-order bandpass filter with triangular microstrip resonators (unit: mm); substrate not shown.

In Fig. 9 the couplings between resonators 1 and 2, 3 and 4, and between resonators 5 and 6 are of electric type while the couplings between resonators 2 and 3 and between resonators 4 and 5 are of magnetic type. The necessary couplings between resonators, given by (3) – (9), determine the position of 50 Ω feeding lines and, also, the gaps between resonators, based on the study in Section 2.

The frequency response of the proposed type 1 filter is shown in the Fig. 10.

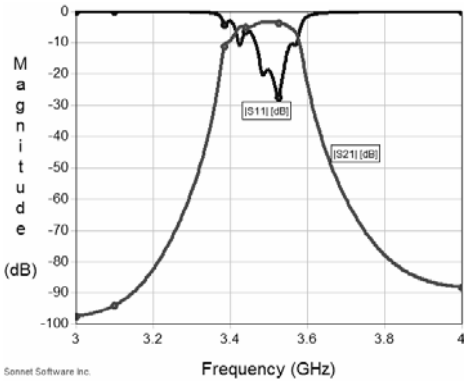

Fig. 10 – Frequency response of the type 1
bandpass filter from Fig. 9.

The electromagnetic-field simulation of the planar structure from Fig. 9 demonstrates a center frequency of 3.492 GHz, an in-band insertion loss of 3.48 dB, a 3 dB bandwidth of 153 MHz, and an in-band return loss of approximately 18.66 dB. These electrical characteristics does not take into account the radiation loss.

It is also noticeable the sharp transitions from passband to stopband provided by the proposed configuration.

Another configuration of microwave bandpass filter with six triangular resonators is given in Fig. 11.

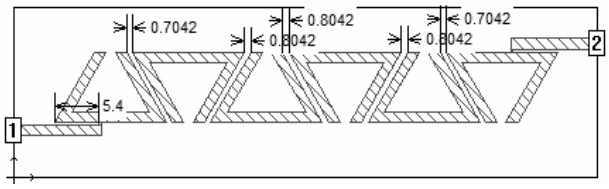

Fig. 11 – Type 2 microwave sixth-order bandpass filter with triangular microstrip resonators (unit: mm); substrate not shown.

Here all six resonators are mixed-coupled, as detailed in the Fig. 5. Compared to the structure from Fig. 9, the type 2 bandpass filter involves a single type of coupling between resonators.

The simulated response of the proposed type 2 bandpass filter from Fig. 11 is shown in the Fig. 12.

The proposed configuration from Fig. 11 has a center frequency of 3.496 GHz, an in-band insertion loss of 3.42 dB, a 3 dB bandwidth of 190 MHz, and an in-band return loss of approximately 11.26 dB.

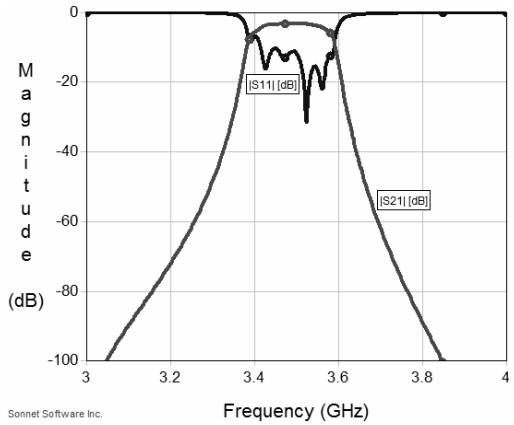

Fig. 12 – Frequency response of the type 2 bandpass filter from Fig. 10.

It is noticed that both filtering structures meet the specification, with small deviation from imposed parameters.

4. EXPERIMANTAL RESULTS

The designed microstrip bandpass filters were fabricated and characterized using an Agilent E5071C vector network analyzer.

The two experimental models are presented in the Fig. 13 and in the Fig. 14 (SMA – F connectors, ground plane not shown).

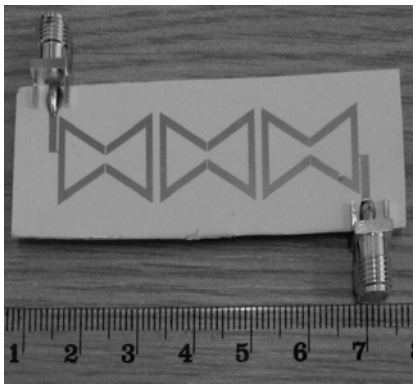

Fig. 13 – Experimental model of the type 1 bandpass filter from Fig. 9.

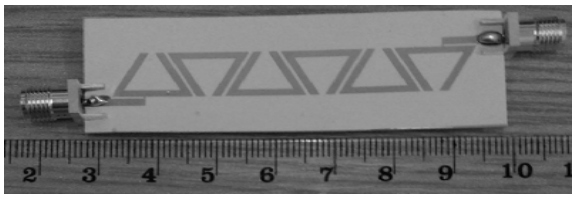

Fig. 14 – Experimental model of the type 2 bandpass filter from Fig. 10.

The measured electrical characteristics of the experimental model from Fig. 13 are shown in the Fig. 15.

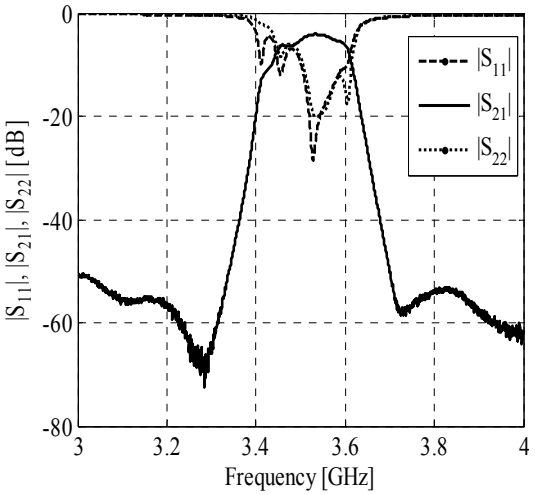

Fig. 15 – The measured frequency response of the experimental model from Fig. 13.

The type 1 bandpass filter from Fig. 13 has a measured center frequency of 3.52 GHz, an in-band insertion loss of 4.28 GHz, a 3 dB bandwidth of 160 MHz, and an in-band return loss of approximately –11.24 dB. Compared to simulated results, the measured ones are influenced by the radiation loss, tolerances of the fabrication process, electrical characteristics of the real SMA connectors, etc.

The measured electrical characteristics of the type 2 bandpass filter from Fig. 14 are presented in the Fig. 16.

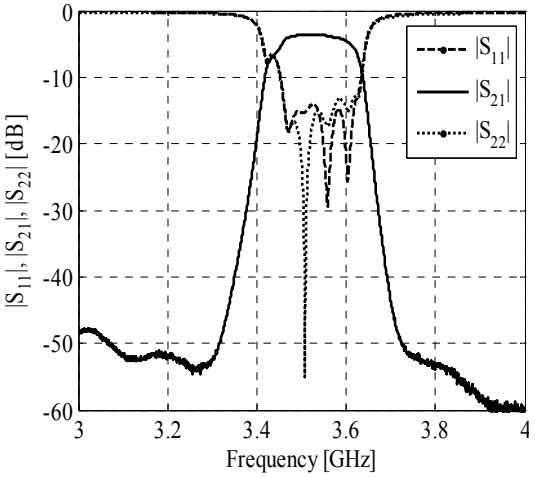

Fig. 16 – The measured frequency response of the experimental model from Fig. 14.

The measured type 2 electrical parameters demonstrate a center frequency of 3.52 GHz, an in-band insertion loss of 3.64 dB, a 3 dB bandwidth of 185 MHz, and an in-band return loss of approximately –14.35 dB.

The electrical parameters of the experimental models from Fig. 13 and Fig. 14 were also measured in a larger frequency range, within (0.5 – 8.5) GHz. The measured frequency responses are depicted in Fig. 17 and Fig. 18, respectively.

First spurious response of the filter from Fig. 13 occurs at 7.22 GHz, in its upper stopband, as can be seen in the Fig. 17. At this frequency, the attenuation has its lowest value, of –22.06 dB.

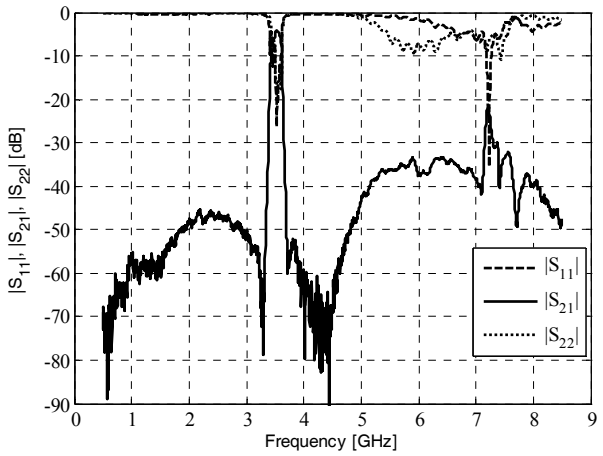

Fig. 17 – The measured frequency response of the experimental model from Fig. 13, within (0.5 – 8.5) GHz frequency range.

From Fig. 18 it can be noticed a similar frequency behavior with the response shown in the Fig. 17. First spurious response of the filter from Fig. 14 appears at 7.33 GHz, with a very poorly attenuation in the upper stopband, of only –8.08 dB.

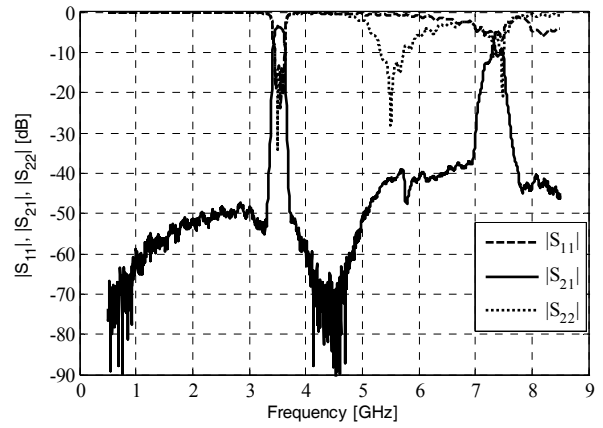

Fig. 18 – The measured frequency response of the experimental model from Fig. 14, within (0.5 – 8.5) GHz frequency range.

In order to evaluate the phase nonlinearity of the proposed filters' S_{21} transfer characteristics, the group delay time of each bandpass filter was measured. The results are graphically depicted in the Fig. 19 and in the Fig. 20.

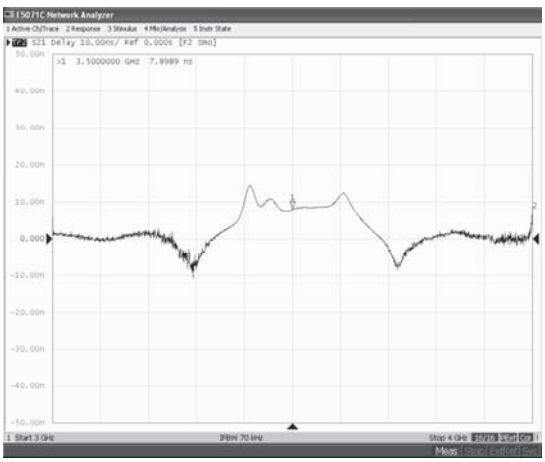

Fig. 19 – Measured group delay time of the bandpass filter from Fig. 13.

As displayed in the Fig. 19, the experimental model of the bandpass filter from Fig. 13 shows an approximately constant group delay time in the filter's passband, of 7.89 ns.

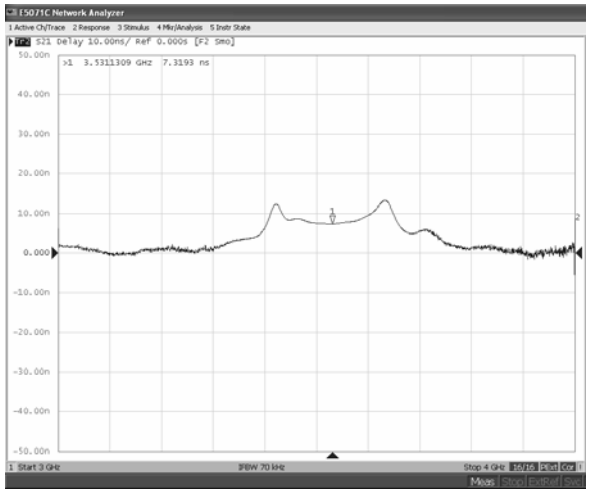

Fig. 20 – Measured group delay time of the bandpass filter from Fig. 14.

The measured group delay time of the bandpass filter from Fig. 14 has an approximately constant value in the filter's passband, of 7.32 ns, as can be seen in the Fig. 20.

5. **CONCLUSIONS**

Two different topologies of microwave bandpass filters with novel triangular open-loop microstrip resonators have been demonstrated. Despite their high order, both filters are characterized by small physical dimensions (7 cm × 2.5 cm filter from Fig. 13, 7 cm × 2 cm filter from Fig. 14) and very good electrical performance: low in-band insertion loss, sharp passband to stopband transitions, and high stopband attenuation up to around twice of their center frequency where first unwanted response occurs. Using a stepped impedance resonator (SIR) geometry [17–19] for the proposed triangular resonator, the frequency behavior of the filters in their upper stopband can be improved, so that, in this case, first spurious response will occur at a frequency higher than twice of the center frequency of the filters. The group delay time of both experimental models is approximately constant in the filters' passband, of around 7 ns.

Further investigation will be focused on designing planar bandpass filters with triangular resonators in a three-metallization layer technology, using apertures etched in the common ground plane as coupling mechanism between resonators located on different metallization layers.

ACKNOWLEDGEMENTS

This work has been funded by "Politehnica" University of Bucharest, through the "Excellence Research Grants" Program, UPB – GEX. Identifier: UPB – Excelență – 2016 Research project title "Innovative microwave filtering structures for telecommunication and radar applications", Contract number 102/26.09.2016.

Received on September 2, 2017

REFERENCES

1. J.-S. Hong, *Microstrip filters for RF/Microwave applications*, John Wiley & Sons, Inc., Hoboken, New Jersey, 2011, pp. 202–228.
2. Y. Heng, X. Guo, B. Cao, *et al*., *Dual-band superconducting bandpass filter with embedded resonator structure*, Electronics Letters, **49**, *17*, pp. 1096–1097 (2013).
3. A. Alburaikan, M. Aqeeli, G.N. Jawad, A. Biswas, Z. Hu, *High selectivity microstrip bandpass filter using feedback CRLH-TL unit cell*, Asia-Pacific Microwave Conference (APMC 2016), New Delhi, India, Dec. 5–9, 2016.
4. H. Shaman, S. Almorqi, O. Haraz, S. Alshebeili, *Hairpin microstrip bandpass filter for millimeter-wave applications*, Mediterranean Microwave Symposium (MMS 2014), Marrakech, Morocco, Dec. 12–14, 2014.
5. P. Castillo-Aranibar, P. Rodriguez-Postigo, D. Segovia-Vargas, *Compact triplexer with open ring resonators as microstrip trisection bandpass filters for asymmetric response*, Microwave & Optoelectronics Conference (IMOC2013), Rio de Janeiro, Brazil, Aug. 4–7, 2013.
6. J. Yang, Z.-Y. Liu, Z.-W. Wang, *Triple-Mode Ring Resonator Microstrip Bandpass Filter with Enhanced Rejection*, Wireless Communication and Sensor Network Conference, Wuhan, China, Dec. 13–14, 2014.
7. S.A. Khodenkov, N.M. Boev, *The investigation of microstrip bandpass filters with wide stop band*, Actual Problems of Electron Devices Engineering (APEDE 2016), Saratov, Russia, Sep. 22–23, 2016.
8. P.-L. Huang, T.-Y. Hsieh, C.-W. Tang, *A design of the compact microstrip bandpass filter with a wide passband and broad stopband*, International Microwave Symposium (IMS2016), San Francisco, CA, USA, May 22–27, 2016.
9. C.-N. Liu, C.-H. Teng, C.-W. Tang, *Design of the wide stopband microstrip bandpass filter by cascading stepped coupled lines*, Asia-Pacific Microwave Conference (APMC 2014), Sendai, Japan, Nov. 4–7, 2014.
10. S. Yang, D. Cross, M. Drake, *Design and simulation of a parallel-coupled microstrip bandpass filter*, IEEE SOUTHEASTCON 2014, Lexington, KY, USA, Mar. 13–16, 2014.
11. S. Neethu, S.S. Kumar, *Microstrip Bandpass Filter Using Fractal Based Hexagonal Loop Resonator*, Cochin, India, Aug. 27–29, 2014.
12. S. Vegesna, M. Saed, *Miniaturized microstrip bandpass filter with interdigitated fingers*, Antennas and Propagation Society International Symposium (APSURSI2013), Orlando, FL, USA, Jul. 7–13, 2013.
13. V.M. Dabhi, V.V. Dwivedi, *Parallel coupled microstrip bandpass filter designed and modeled at 2 GHz*, Signal Processing, Communication, Power and Embedded System Conference (SCOPES2016), Paralakhemundi, India, Oct. 3–5, 2016.
14. Y.-D. Chen, C.-H. Liu, *Exploiting Hi-Lo inter-digital DGS for high-order microstrip bandpass filters*, Antennas and Propagation Asia-Pacific Conference (APCAP2016), Kaohsiung, Taiwan, Jul. 26–29, 2016.
15. Sonnet Software Inc., *Sonnet Professional ver. 16.52*, NY, USA, www.sonnetsoftware.com (2017).
16. Ansys Inc., *Ansoft Designer SV 2.2*, USA, www. ansys.com (2005).
17. Z. Li, W. Shi, Y. Yuan, *A novel compacted microstrip bandpass filter using stepped impedance resonator (SIR) and defected ground structure (DGS)*, Electronic Packaging Technology Conference (ICEPT2014), Chengdu, China, Aug. 12–15, 2014.
18. C.-W. Tang, W.-M. Chuang, *Design of a compact dual-band bandpass filter with DGS-SIR resonators*, Asia-Pacific Microwave Conference (APMC2015), Nanjing, China, Dec. 6–9, 2015.
19. H. Aouidad, J.-F. Favennec, E. Rius, A. Manchec, Y. Clavet, *A tunable filter based on miniature SIR coaxial resonators*, European Microwave Conference (EuMC2015), Paris, France, Sept. 7–10, 2015.